Journal of Solid Mechanics Vol. 8, No. 2 (2016) pp. 435-445

# Seismic Analysis of Rectangular Concrete Tanks by Considering Fluid and Tank Interaction

M. Yazdanian [1,*], S.V. Razavi [2], M. Mashal [3]

[1] *Department of Civil Eengineering, Dezful Branch, Islamic Azad University, Dezful, Iran*
[2] *Department of Civil Engineering, Jundi-Shapur University of Technology, Dezful, Iran*
[3] *Department of Irigation Engineering, Aburaihan Campus, Tehran University, Tehran, Iran*

Received 23 March 2016; accepted 20 May 2016

**ABSTRACT**

Many liquid storage tanks around the world have affected by earthquakes. This structure can store dangerous chemical liquids. Hence dynamic behavior of ground supported rectangular storage tanks is very important due to their applications in industrial facilities. In current research, the seismic behavior of two water storage rectangular concrete tanks is examined. For this purpose, these tanks are modeled in FEM software for analyzing. These tanks are analyzed under four type of analysis: static, modal, response-spectrum and time-history analysis. Time history analysis can take all the nonlinear factors into the analysis, so it is used to estimate the exact amount of structural response. In time history analysis, earthquake accelerograms of Tabas, Kobe and Cape Mendocino have been applied to tanks. Finally, it is resulted that Displacement, base shear and wave height obtained from time history analysis are more than those of response spectrum analysis, indicating insufficiency of response spectrum analysis. In time history analysis, the maximum displacement is achieved in highest part of the tanks. It is due to the wave height which created in earthquake. By increasing in dimension, the wave height is also increased.



**Keywords :** Rectangular tank; Earthquake; Time history; Accelerograms; Wave height.

## 1 INTRODUCTION

RECTANGULAR concrete tanks are widely applied as engineering structures to store water, fuel or the other liquids. Earthquake behavior of storage tanks is very different of other structure. This is due to liquid-structure interaction of the system. In the liquid- structure interaction systems, liquid significantly affect response of the structure under earthquake loads [1]. The destroying effects of the earthquakes make the problem more confusing compared to the static design method for liquid storage tanks. Hence, the stability of the liquid storage tanks under earthquake conditions must be studied carefully. The wall movement causes distortion or even breakdown of the system [2]. Failure of storage tanks along earthquakes may have effects on public safety. Storage tanks as lifeline and strategically important structures have use in many facilitates. Destruction of this structure may lead to fires or environmental contaminations due to flammable materials or hazardous chemicals leakage pollution. This is due to liquid-structure interaction of the system. [3]. on August 17, 1999 a magnitude 7.4 earthquake that occur Turkey caused to collapse of a 115 m-high reinforced concrete chimney or heater stack located at the largest oil refinery in Turkey and other industrial facilities [4]. More information about this earthquake and tanks which have damaged are

[*] Corresponding author. Tel.: +989163197453.
*E-mail address: Yazdanian.mohsen@yahoo.com* (M. Yazdanian).

investigated by some research [5-7]. For the first time, the dynamic behavior of the tanks is investigated by Housner [8, 9]. In this method hydrodynamic pressure is divided into impulsive and convective part using lumped mass approximation. The Housner's model has been selected for dynamic analysis of tanks in all of codes and standards. Edwards [10] proposed a FEM method to be used for estimating the seismic performance of deformable liquid storage tanks. A cylindrical liquid storage tank with the height to diameter ratio of less than one was examined using the finite element method. The suggested FEM model was capable of accounting for the coupled interaction between the stored liquid and the elastic tank shell. An expanded application of Housner's method, in the terms of a practical design rule, was given by Epstein [11]. For rectangular tanks, Haroun [12] suggested a very comprehensive model for analysis on the general system of loadings of tanks. The hydrodynamic pressures were computed by a classical potential flow method. The formulation of hydrodynamic pressures just regarded the rigid wall condition. This may be because of that rectangular concretet tanks are generally made of reinforced concrete and may be regarded entirely rigid. Haroun and Tayel [13] proposed a FEM model for analyzing the dynamic response of liquid storage tanks. Rosenblueth and Newmark [14] proposed a lumped mass model for rigid liquid storage tanks and obtained their seismic response. Later, Veletos and Yang [15] studied the effects of wall type on the pressure distribution in liquid and corresponding forces in the tank structure through an analytical model. Park et al. [16] employed the coupled boundary-finite element technique to study response of rectangular tanks. Chen and Kianoush [17] presented a model called sequential method for determining the hydrodynamic pressure values in CRST in a two dimensional space. In the proposed method, the effect of wall flexibility was also contained. Virella et al [18] studied on the natural periods, mode shapes, and dynamic response to ground motion of cylindrical tanks partially filled with a liquid. The contained liquid was modeled using the added mass formulation and acoustic liquid elements based on linear wave theory without any sloshing in waves. Ozdemir et al [19] analyzed the steel cylindrical storage tanks using nonlinear methods for fluid–structure interaction in the Finite Element Method. Also they studied experimental on anchored and unanchored tanks for the verification of the accuracy of the numerical procedure. The numerical methods, especially the finite element method, have been widely applied for replicating actual physical behavior of the tanks. More research on the behavior of tanks under dynamic loads can be investigated by [20-23]. Most research is performed on cylindrical tanks. However there are some researches on seismic behavior of rectangular tanks. So in current research, a comprehensive study is performed on two rectangular concrete tanks. These tanks are analyzed under four type of analysis: static, modal, response- spectrum and time-history analysis.

## 2 MATHEMATICAL MODEL

In the Eulerian and Lagrangian methods, the governing fluid structure system equation is calculated using wave propagation through the fluid by assuming linear compressibility and inviscousity. The wave propagation equation through fluid is as follow [24]:

$$\nabla^2 p = \frac{1}{c^2}\frac{\partial^2 p}{\partial t^2} \tag{1}$$

where, $p$ is the acoustic pressure in the fluid at time ($t$) and $c$ is the acoustic wave speed. The continuity condition of contained fluid in this theory is consisted of boundary conditions of the contact interface between tank body and fluid as well as fluid free surface. The fluid is assumed to be, irrotational, incompressible and inviscid and also there is no mean flow of the fluid. Furthermore, the linear theory of sloshing is utilized for the convective response of the contained liquid in tank. The velocity of pressure wave assumed to be infinity in the small volume of containers. So the wave equation of the fluid system can be considered as following in three-dimensional space by assuming an ideal fluid [23], [24]:

$$\nabla^2 p(x,y,z,t) = 0 \tag{2}$$

In which, $p = p(x,y,z,t)$ is the hydrodynamic pressure. To discretize the wave equation within fluid domain, first the following matrix operators (gradient and divergence) are introduced:

$$\{\nabla.(\ )\} = \{L\}^T = \left[\frac{\partial}{\partial x}\frac{\partial}{\partial y}\frac{\partial}{\partial z}\right] \tag{3}$$

$$\nabla(\ ) = \{L\} \tag{4}$$

Therefore, Eq. (2) can be rewritten in matrix notation as:

$$\{L\}^T(\{L\}p) = 0 \tag{5}$$

The hydrodynamic pressure *p* in this equation could be because of horizontal and vertical dynamic excitations of the tank walls and floor. Dynamic motions at these boundaries are related to the hydrodynamic pressure in fluid domain by defining proper boundary conditions along structure– fluid interfaces as follows:

$$\frac{\partial p(x,y,z,t)}{\partial n} = -\rho_l a_n(x,y,z,t) \tag{6}$$

or in matrix notation as:

$$\{n\}^T(\{L\}p) = -\rho_l\{n\}^T\left[\frac{\partial^2}{\partial t^2}\{u\}\right] \tag{7}$$

where, $\rho_l$ is the liquid density; $a_n$ is the acceleration component on the boundary along the direction outward normal n; $\{n\}$ is the unit normal to the interface S; $\{u\}$ is the displacement vector of the structure at the interface and t is the time.

The following boundary condition accounting for the sloshing effects can be written based on the small amplitude wave assumption on the fluid free surface:

$$\frac{1}{g}\frac{\partial^2 p}{\partial t^2} + \frac{\partial p}{\partial z} = 0 \tag{8}$$

In which, *g* represents the acceleration due to gravity and *z* is the vertical direction. By utilizing the boundary condition mentioned in Eq. (8), the convective pressure distribution within the fluid domain can be achieved. The mentioned boundary condition at fluid free surface should be replaced with the following boundary condition which imposes zero impulsive pressure at the free surface, by considering impulsive component of the fluid response. At $z = H_1$ (liquid free surface)

$$p(x,y,z,t) = 0 \tag{9}$$

In which, $H_1$ is the height of the stored liquid. The discretized for a multi degree of freedom system subjected to external dynamic forces can be defined as [25]:

$$[M]\{\ddot{u}\} + [C]\{\dot{u}\} + [K]\{u\} = \{f^a\} \tag{10}$$

where:

$[M]$, is the mass matrix of the system

$[C]$ , is the damping matrix of the system

$[K]$ , is stiffness matrix of the system

$\{u\}$, is displacement vector

$\{\dot{u}\}$, is velocity vector

$\{\ddot{u}\}$, is acceleration vector

$\{f^a\}$, is the applied load vector

The interaction between the tank structure and contained fluid causes a hydrodynamic pressure which applies a force on the structure and so created structural motions produce an effective fluid load. In order to obtain the structure- fluid coupling equations, $\{f^a\}$ in Eq. (10) consists of resultant of all other forces $\{f_e\}$ and the fluid pressure load acting at the interface $\{f_e^{pr}\}$, following equations is introduced by [23]:

$$[M_e]\{\ddot{u}_e\}+[C_e]\{\dot{u}_e\}+[K_e]\{u_e\}=\{f_e\}+\{f_e^{pr}\} \tag{11}$$

The fluid pressure load acting at the interface of structure- fluid interface (*s*) can be calculated by integrating the pressure over the interface surface area as:

$$\{f_e^{pr}\}=\int_s \{G'\}p\{n\}\,d(s) \tag{12}$$

In which, $\{G'\}$ is the shape functions used to discretize the structural displacement components (obtained from the structural element), *p* is the fluid pressure, and $\{n\}$ is the normal at the fluid boundary. Using the finite element approximating shape functions for the spatial variation of the fluid pressure, one can write:

$$p=\{G\}^T\{p_e\} \tag{13}$$

In which, $\{G\}$ is the shape function for fluid in pressure, and $\{p_e\}$ is the nodal pressure vector. By substituting Eq. (13) into Eq. (12) gives:

$$\{f_e^{pr}\}=\int_s \{G'\}\{G\}^T\{n\}\,d(s)\{p_e\} \tag{14}$$

The fluid pressure load can be defined as Eq. (15) by definition of coupling matrix $[R_e]$ relates the pressure of the fluid and the forces on the structure-fluid interface.

$$\{f_e^{pr}\}=[R_e]\{p_e\} \tag{15}$$

By comparing the Eqs. (14) and (15), the coupling matrix is found to be:

$$[R_e]^T=\int_s \{G'\}\{G\}^T\{n\}\,d(s) \tag{16}$$

By substituting Eq. (15) into Eq. (11), the dynamic elemental equation of the structure is obtained as:

$$[M_e]\{\ddot{u}_e\}+[C_e]\{\dot{u}_e\}+[K_e]\{u_e\}-[R_e]\{p_e\}=\{f_e\} \tag{17}$$

## 3 FINITE ELEMENT MODELING

The motion equation, Eq. (10) and the wave equation, Eq. (1) have to be mentioned all together in finite element achievement to simulate the structure– fluid interaction problem.

The total hydrodynamic response can be calculated from the wave equation Eq. (1), as well as the proper boundary conditions as mentioned in Eqs. (6) and (8). The impulsive part of response can be finding by replacing the boundary condition defined in Eq. (8) with the boundary condition in Eq. (9). Having obtained the total and impulsive response values, the convective response is the difference between these two values. Employing the finite element shape functions for the spatial variation of the displacement components u within the structural domain, the following equation can be written [23]:

$$u = \{G'\}^T \{u_e\} \tag{18}$$

In which, $\{u_e\}$ is the nodal displacement component vector. For simplicity in deriving the equations, the following notation can be introduced:

$$[C] = \{L\}\{G\}^T \tag{19}$$

Finally, using previously mentioned boundary conditions in finite element discretization, the discretized wave equation in matrix notation can be defined:

$$\left[M_e^p\right]\{\ddot{p}_e\} + \left[K_e^p\right]\{p_e\} + \rho_l [R_e]^T \{\ddot{u}_e\} = \{0\} \tag{20}$$

where:

$$\left[M_e^p\right] = \frac{1}{g}\int_{fs} \{G\}\{G\}^T d(fs)\ ,\ \left[K_e^p\right] = \int_{vfe} [C]^T [C] d(vfe)\ ,\ [R_e] = \int_{s} \{G\}\{n\}^T \{G'\}^T d(s)$$

In above equations, ‘‘*fs*’’ and ‘‘*vfe*’’ express free surface and volume of the fluid element, respectively. As mentioned before, *s* indicates structure-fluid interface. Waste of energy because of the fluid damping can be computed by adding a waste term to the above equation:

$$\left[M_e^p\right]\{\ddot{p}_e\} + \left[C_e^p\right]\{\dot{p}_e\} + \left[K_e^p\right]\{p_e\} + \rho_l [R_e]^T \{\ddot{u}_e\} = \{0\} \tag{21}$$

In which, $\left[C_e^p\right]$ is the matrix representing the damping in fluid. In this research, similar classical damping system said as Rayleigh damping ( $\alpha$ and $\beta$ ) is applied for both structural and fluid domains leading to a classical damping for the whole scheme. Alpha damping and Beta damping are applied to indicate Rayleigh damping constants $\alpha$ and $\beta$ . The damping matrix within the fluid domain $\left[C_e^p\right]$ contains two parts which are because of impulsive and convective components of the stored fluid:

$$\left[C_e^p\right] = \alpha[M] + \beta[K] + \sum_{i=1}^{m}[CFi] \tag{22}$$

$\alpha$ is defined based on the natural frequency of the primary sloshing mode and calculates for the damping because of sloshing on the free surface of the tank liquid. $\beta$ is defined based on the primary frequency of the tank and simulates the damping because of the impulsive part. As offered by ACI 350.3-06 [26], damping ratios of 5% and 0.5% are specified for the impulsive and convective parts, respectively. Two modes of $\omega_i, \omega_j$ are the impulsive and convective modes which are achieved from modal analysis according to maximum effective mass.

$$\begin{bmatrix}\alpha\\ \beta\end{bmatrix} = \frac{2\omega_i\omega_j}{\omega_j^2+\omega_i^2}\begin{bmatrix}\omega_j & -\omega_i\\ -\dfrac{1}{\omega_j} & \dfrac{1}{\omega_i}\end{bmatrix}\begin{bmatrix}\xi_i\\ \xi_j\end{bmatrix} \tag{23}$$

The time history response of the structure-fluid system is calculated using direct integration method. By defining the displacement and hydrodynamic pressure at time increment I, the displacement and hydrodynamic pressure values at time increment $i+1$ can be calculated using the direct integration system. In this method, the step by step integration is applied directly to achieve the solution for the original equations of motion of the system. The finite difference expansions in the time interval $\Delta t$ in Newmark time integration method is used for the solution of Eq. (21). In the current research, an integration time step of 0.02s is applied to the systems. ANSYS [27] as general purpose computer code is utilized to perform FEM analyses [23]. ANSYS [27] software is used for the finite element modeling, wherein, the container wall and the base is modeled using the SOLID65 element. This element is used for the 3-D modeling of concrete. The fluid is modeled using FLUID80 element. This element is particularly well suited for calculating hydrostatic pressures and fluid/solid interactions.

The properties of material of tank and liquid of container are shown in Table 1. And also the geometric characteristics of the selected tanks are shown in Table 2. For parametric analysis, two tanks are selected. These tanks are filled with fluid of water.

**Table 1**
Properties of liquid and tank for concrete rectangular tanks.

| Material type | density(kg/m^3) | Poisson's ratio | Young's modulus (Gpa) |
|---|---|---|---|
| concrete | 2500 | 0.2 | 25 |
| water | 1000 | - | 2.07 |

**Table 2**
Characteristics of the selected tanks.

| Tank number | length (m) | Height (m) | wide (m) | Fluid height (m) | Wall thickness (m) | Foundation thickness (m) |
|---|---|---|---|---|---|---|
| 1 | 9.5 | 3 | 6.2 | 2.5 | 0.3 | 0.35 |
| 2 | 11.3 | 3 | 11.3 | 2.5 | 0.35 | 0.4 |

Finite element modeling of these two tanks is illustrated in Figs. (1,2). As evident, these tanks have regular elements. Regular elements have a strong influence on the results.

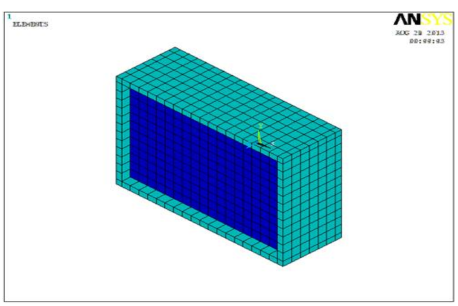

**Fig.1**
Finite element modeling of tank No.1.

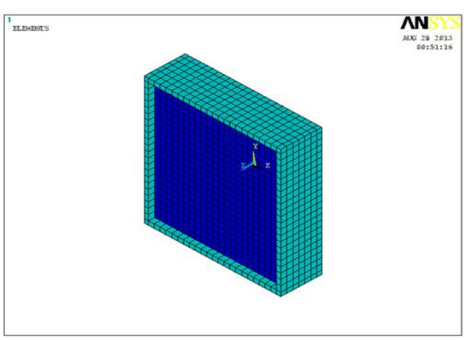

**Fig.2**
Finite element modeling of tank No.2.

## 4 RESULTS
### *4.1 Static analysis*

In first step, the tanks were analyzed based on their weight and the hydrostatic pressure of internal fluid. This analysis can be used in compound loading, and also it can be used as a criterion for the evaluation of constructed model. The generated hydrostatic pressure causes annular tensile stresses in the tank wall. A summary of the main results of this analysis is presented in Table 3.

By comparing results in static analysis, it is observed that the tanks no.1 has the more displacement than tank No.2. The tank No.2 has the more volume of fluid inside itself but this tank has a more wall thickness than tank No.1. So tank No.1 has the more displacement.

**Table 3**
Maximum results in static analysis.

| Tank No | Displacement (m) | Tensile stress (Mpa) |
|---|---|---|
| 1 | 0.0005 | 0.856 |
| 2 | 0.0004 | 0.698 |

### *4.2 Modal analysis*

Natural frequencies and mode shapes of a tank are important parameters in the analysis of tank. Determining these parameters in the first step can be very useful in interpreting the behavior of the tank. Convective and impulsive modes are most important modes which have the maximum effective mass to account for the dynamic analysis. According to the maximum effective mass in modal analysis two modes of impulsive and convective are extracted and these modes amount are set in Eq. (23). In addition, this analysis can be a starting point for other analysis, such as response spectrum analysis or time history analysis. Fig. 3 illustrates two vibrational modes of the tank No.1, 2.

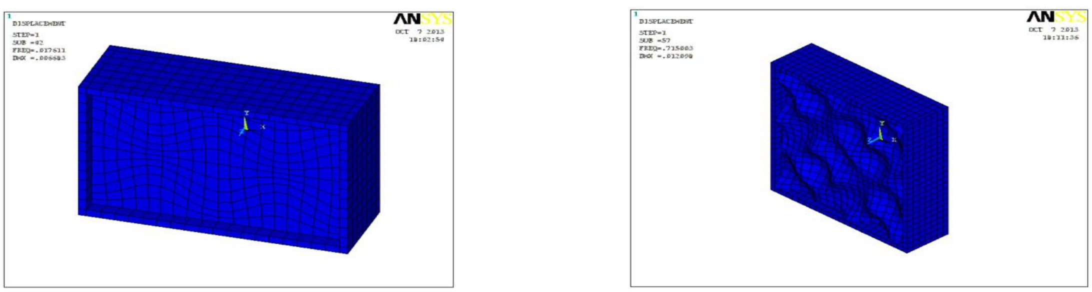

**Fig.3**
Vibration mode of tanks No 1, 2.

### *4. 3 Response spectrum analysis*

After modal analysis and determination of main tank modes, response spectrum analysis was performed. A three component site design spectrum for area soil with moderate earthquake hazard has entered into tanks. According to Standard No. 2800 [28] Site design spectrum is defined. CQC method is used for combining the modes. By comparing result, it is observed that by increasing in length and wide the height wave will increase.

In the Figs. (4,5), maximum tensile stress in response spectrum analysis is illustrated. It is observed that the maximum stress is achieved in the corner of the tanks and lower part of the tank. This is due to the hydrodynamic pressure which exerted to the walls. Also maximum height wave is achieved in the corner of the tanks. This wave height is illustrated in Figs. (6,7) due to the wave height is achieved in corner of the tanks, so the maximum stress is achieved in corner of the tanks. And the pressure of the fluid in corner and lowest part of the tank is more than other parts. Also it is observed that the minimum height wave is achieved in center of the tanks.

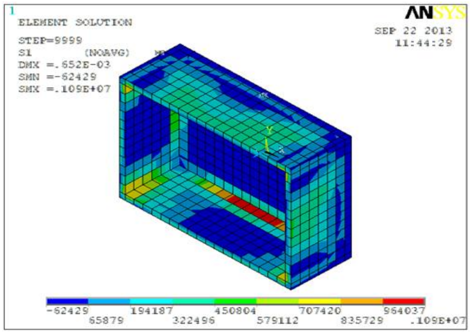


**Fig.4**
Maximum stress in the wall of tank No.1.

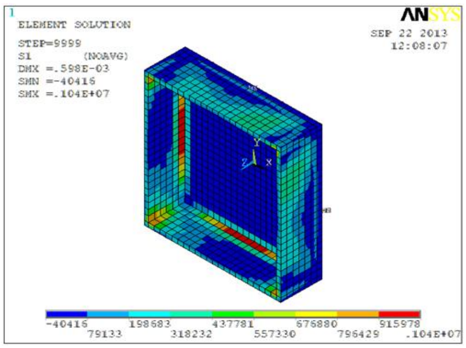


**Fig.5**
Maximum stress in the wall of tank No.2.

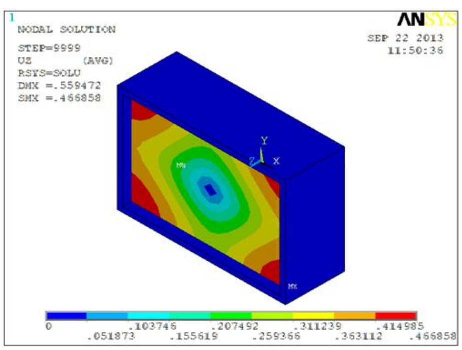


**Fig.6**
Maximum wave height in tank No.1.

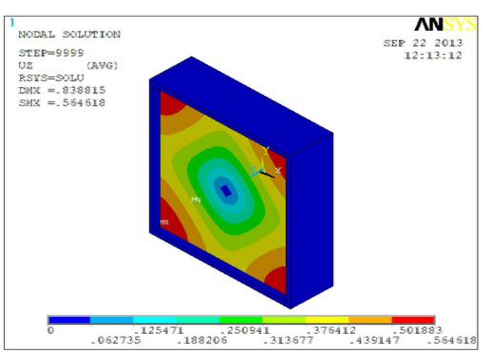


**Fig.7**
Maximum wave height in tank No.2.

*4.4 Time history analysis*

Time history analysis can take all the nonlinear factors into the analysis, so it is used to estimate the exact amount of structural response. In time history analysis, earthquake accelerograms of Tabas, Kobe and Cape Mendocino have been applied to tanks. The results obtained from maximum base shear are shown in Table 4. Detailed study of base shear of tanks show that the maximum base shears values is obtained in Tabas earthquake which is due to more PGA of Tabas earthquake than other two. Tank No. 2 due to its heavy weight shows a greater base shear than other tanks. In every 0.02 seconds, the maximum base shears of the bottoms nodes are assembled together.

**Table 4**
Maximum base shear of the tanks (MN).

| Tank No | Earthquake name | Longitude Base shear | Transverse base shear | Vertical base shear |
|---|---|---|---|---|
| | Tabas | 0.714 | 0.936 | 0.987 |
| 1 | Kobe | 0.515 | 0.846 | 0.719 |
| | Cape Mendocino | 0.638 | 0.84 | 0.736 |
| | Tabas | 1.45 | 1.59 | 1.79 |
| 2 | Kobe | 1.028 | 1.08 | 1.39 |
| | Cape Mendocino | 1.14 | 1.2 | 1.41 |

The maximum longitude Base shear in tank No.1, 2 under Tabas Earthquake is shown in Figs. 8 and 9. The maximum base shear in tank No.1, 2 is achieved in 10.48 seconds after the earthquake. The value of the maximum base shear of the tanks can be estimated in every 0.02 seconds of the earthquake.

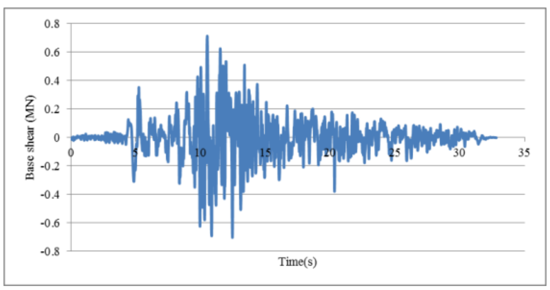


**Fig.8**
Maximum longitude base shear in tank No.1 under Tabas earthquake**.**

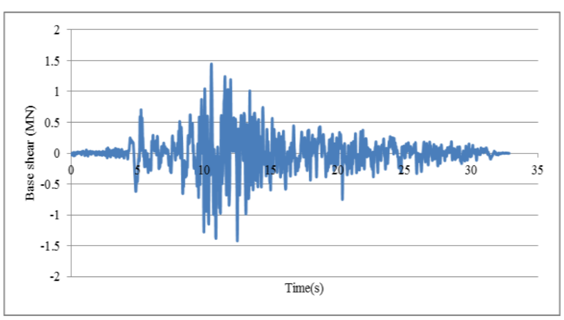


**Fig.9**
Maximum longitude base shear in tank No.2 under Tabas earthquake.

Maximum displacements of tanks are shown in Table 5. It is resulted that the displacement in tank No.1 is more than tank No.2. Also the most displacements in both tanks is achieved in highest part of the tanks. This is due to the pressure of wave height which exerted to the upper layer of the wall.

**Table 5**
Maximum displacement of the tank wall (m).

| Tank No | Earthquake name | Longitude displacement | Transverse displacement | Vertical displacement |
|---|---|---|---|---|
| 1 | Tabas | 0.0004 | 0.001 | 0.00006 |
| | Kobe | 0.0003 | 0.0007 | 0. 00006 |
| | Cape Mendocino | 0.0004 | 0.001 | 0. 00004 |
| 2 | Tabas | 0.0008 | 0.0008 | 0.00007 |
| | Kobe | 0.0007 | 0.0006 | 0.00006 |
| | Cape Mendocino | 0.0009 | 0.0009 | 0.00007 |

In Table. 6, the maximum wave height of tanks is presented. It is resulted that the maximum wave height is occurred in TABAS earthquake. It is due to PGA of this earthquake is more than the others. Also wave height in tank No.2 is more than the wave height in tank No.1. It is due to the dimension of this tank is bigger than tank No.2.

**Table 6**
Maximum wave height (m).

| Tank No | Earthquake name | Wave height |
|---|---|---|
| 1 | Tabas | 1.08 |
| | Kobe | 0.9 |
| | Cape Mendocino | 1 |
| 2 | Tabas | 1.12 |
| | Kobe | 0.93 |
| | Cape Mendocino | 1.04 |

## 5 CONCLUSIONS

In current research, two rectangular concrete tanks are modeled in FEM software and four type of analysis are done in these tanks. The most important result is stated as follow:

Displacement, base shear and wave height obtained from time history analysis are more than those of response spectrum analysis, indicating insufficiency of response spectrum analysis.

Studying the impact of different values on the PGA on seismic performance of tanks determined that more PGA, the results as of base shear, displacement and wave height increases in tank.

In time- history analysis, the maximum displacement is achieved in highest part of the tanks. It is due to the wave height which created in earthquake.

The maximum stresses are achieved in the lowest part of the tanks and in the corner of the tanks.

By increasing in dimension, the wave height is also increased. This is observed in both Time history and response- spectrum analysis.

The thickness of the wall has a very important effect in the behavior of the tanks. It is observed the tanks which have the greater dimension, but have bigger thickness wall tolerated less displacement.

The tank which has the greater weight has the bigger base shear. Also the PGA of the earthquake has a strong effect on increasing of base shear.

## ACKNOWLEDGEMENTS

The authors would like to express their appreciation to the Nation Iranian South Oil Company for financial support and the necessary facilities to conduct this research.

## REFERENCES


[1] Bayraktar A., Sevim B., Altunışık A., Türker T ., 2010, Effect of the model updating on the earthquake behavior of steel storage tanks, *Journal of Constructional Steel Research* **66** (3): 462-469.

[2] Livaoglu R., 2008, Investigation of seismic behavior of fluid–rectangular tank–soil/ foundation systems in frequency domain, *Soil Dynamics and Earthquake Engineering* **28**: 132-146.

[3] Shekari M., Khaji N., Ahmadi M., 2010, On the seismic behavior of cylindrical base-isolated liquid storage tanks excited by long-period ground motions, *Soil Dynamics and Earthquake Engineering* **30**(10): 968-980.

[4] Sezen H., Livaoglu R., Dogangun A., 2008, Dynamic analysis and seismic performance evaluation of above-ground liquid containing tanks, *Journal of Structural Engineering* **30**: 794-803.

[5] Sezen H., Whittaker A.S., Elwood K.J., Mosalam K.M., 2003, Performance of reinforced concrete and wall buildings during the August 17, 1999 Kocaeli, Turkey earthquake, and seismic design and construction practice in Turkey, *Journal of Structural Engineering* **25** (1):103-114.

[6] Sezen H., Whittaker A.S., 2004, Performance evaluation of industrial facilities during the 1999 Kocaeli, Turkey earthquake, *Proceedings of the 13th World Conference on Earthquake Engineering*, Vancouver, Canada.

[7] Korkmaz K.A., Sari A., Carhoglu A.I., 2011, Seismic risk assessment of storage tanks in Turkish industrial facilities, *Journal of Loss Prevention in the Process Industries* **24**(4): 314-320.

[8] Housner G.W., 1957, Dynamic pressures on accelerated fluid containers, *Bulletin of the Seismological Society of America* **47**(1): 15-37.

[9] Housner G.W., 1963, The dynamic behavior of water tanks, *Bulletin of the Seismological Society of America* **53**(2): 381-387.

[10] Edwards N., 1969, A procedure for the dynamic analysis of thin walled cylindrical liquid storage tanks, Ph.D Thesis, Ann Arbor (MI), University of Michigan.

[11] Epstein H.I., 1976, Seismic design of liquid storage tanks, *Journal of the Structural Division ASCE* **102**: 1659-1673.

[12] Haroun M.A., 1984, Stress analysis of rectangular walls under seismically induced hydrodynamic loads, *Bulletin of the Seismological Society of America* **74**(3):1031-1041.

[13] Haroun M.A., Tayel M.A., 1985, Response of tanks to vertical seismic excitations, *Earthquake Engineering and Structural Dynamic* **13**: 583-595.

[14] Rosenblueth E., Newmark N.M., 1971, *Fundamentals of Earthquake Engineering*, Englewood Cliffs, NJ: Prentice-Hall.

[15] Veletsos A.S., Yang J.Y., 1977, Earthquake response of liquid storage tanks, in advances in civil engineering through engineering mechanics, *Proceedings of the Second Engineering Mechanics Specialty Conference*, *ASCE/EMD Specialty Conference*, Raleigh, NC.

[16] Park J.H., Koh H.M., Kim J., 1990, Liquid-structure interaction analysis by coupled boundary element-finite element method in time domain, *Proceedings of 7th International Conference on Boundary Element Technology*, *BE-TECH/92*, Southampton ,England.

[17] Chen J.Z., Kianoush M.R., 2005, Seismic response of concrete rectangular tanks for liquid containing structures, *Canadian Journal of Civil Engineering* **32**: 739-752.

[18] Virella J.C., Godoy L.A., Suarez L.E., 2006, Fundamental modes of tank-liquid systems under horizontal motions, *Engineering Structures* **28**(10):1450-1461.

[19] Ozdemir Z., Souli M., Fahjan Y.M., 2010, Application of nonlinear fluid–structure interaction methods to seismic analysis of anchored and unanchored tanks, *Journal of Engineering Structures* **32**: 409-423.

[20] Kianoush M.R., Chen J.Z., 2006, Effect of vertical acceleration on response of concrete rectangular liquid storage tanks, *Engineering Structures* **28**(5):704-715.

[21] Livaoglu R., 2008, Investigation of seismic behavior of fluid–rectangular tank–soil/ foundation systems in frequency domain, *Soil Dynamics and Earthquake Engineering* **28**: 132-146.

[22] Kianoush M.R., Ghaemmaghami A.R., 2011, The effect of earthquake frequency content on the seismic behavior of concrete rectangular liquid tanks using the finite element method incorporating soil–structure interaction, *Engineering Structures* **33**: 2186-2200.

[23] Moslemi M., Kianoush M.R., 2012, Parametric study on dynamic behavior of cylindrical ground-supported tanks, *Engineering Structures* **42**: 214-230.

[24] Zienkiewicz O.C., Taylor R.L., Zhu J.Z., 2005, *The Finite Element Method: Its Basis and Fundamentals*, Sixth edition, Published by Elsevier.

[25] Chopra A.K., 2000, *Dynamics of Structures, Theory and Applications to Earthquake Engineering*, Prentice-Hall.

[26] Seismic Design of Liquid-Containing Concrete Structures (ACI 350.3-06) and Commentary (ACI 350.3R-06), 2009, Farmington Hills (MI, USA), American Concrete Institute.

[27] ANSYS, Inc. ANSYS Release 12.0 Documentation, USA.

[28] Iranian Code of Practice for Seismic Resistant Design of Buildings, Standard No. 2800- 84, Building and Housing Research Center.